Ultrahigh-speed silicon-based modulators/photodetectors for optical interconnects

Xiao Hu,[1,2*] Dingyi Wu,[1] Hongguang Zhang,[1] Daigao Chen,[1,2] Lei Wang,[1,2] Xi Xiao,[1,2,3*] and Shaohua Yu[1,2,3]
[1]*National Information Optoelectronics Innovation Center, Wuhan Research Institute of Posts & Telecommunications, 430074 Wuhan, China*
[2]*State Key Laboratory of Optical Communication Technologies and Networks, China Information and Communication Technologies Group Corporation (CICT), 430074 Wuhan, China*
[3]*Peng Cheng Laboratory, Shenzhen 518055, China*
**e-mail address: huxiao@noeic.com, xiaoxi@nocie.com*

Abstract: We present our recent progress on the silicon photonic devices for next-generation optical interconnects. The 300 Gbit/s silicon microring modulator, 200 Gbit/s Ge EAM and 408 Gbit/s Ge-Si photodetector with the highest bandwidth of 110 GHz are presented. Single-chip 1.6 Tbit/s silicon-based optical transceiver is also demonstrated.

1. Introduction

Silicon photonics (SiPh) has been identified as a critical enabling technology for data centers, coherent communication, high-performance computer, and integrated artificial intelligence (AI) circuits applications because of its low cost, small footprint, low power consumption, high bandwidth, and complementary metal oxide semiconductor (CMOS) compatibility [1, 2]. The two key building blocks for silicon photonics are the modulators and photodetectors. For the silicon photonics modulators, the optical modulation is mainly realized by employing silicon (Si) free carrier plasma dispersion effect [3], Ge-Si or pure Ge Franz-Keldysh (FK) or quantum-confined Stark effect [4]. During the modulator design process, it's critical to make compromise between the bandwidth, insertion loss and driving voltage. The typical modulator structure is based on Mach-Zehnder interferometers (MZIs) and resonant cavities (microring resonator-MRM, microdisk). Although the traveling wave electrode (TWE) based modulator possess the operation speed of larger than 300 Gbit/s for single lane [5], its optical loss, footprints, and power consumption still need to be improved. The lumped electrode modulation structure of silicon microring modulator and GeSi-based electro absorption modulator might be a suitable solution for the low-cost and high-speed silicon photonic integrated on-chip optical interconnects. For the SiPh photodetectors (PDs), the germanium (Ge) is the critical materials for O and C+L band optical detection due to its large absorption coefficient. Various waveguide-integrated Ge-Si PDs have been comprehensively investigated [6]. Based on the novel biconcave Ge fin shape, the recorded 3-dB cut-off frequency up to 265 GHz has been reported [7], which is an important milestone. The quantum efficiency and dark current need to be further improved, which is very important for optical large signal detection. The ultrahigh-speed, high responsivity, and low dark current PDs with easy fabrication processes is very helpful for realizing low-cost SiPh integrated on-chip optical interconnects.

In this paper, we present our recent work on the silicon photonic devices for next-generation optical interconnects. The silicon microring modulator, Ge-Si based EAM and Ge-Si photodetectors with the highest bandwidth of 110 GHz and highest data rate of beyond 400 Gb/s is presented. Additionally, the single-chip 1.6 Tb/s silicon-based optical transmitter and receiver is also demonstrated.

2. Silicon microring modulator

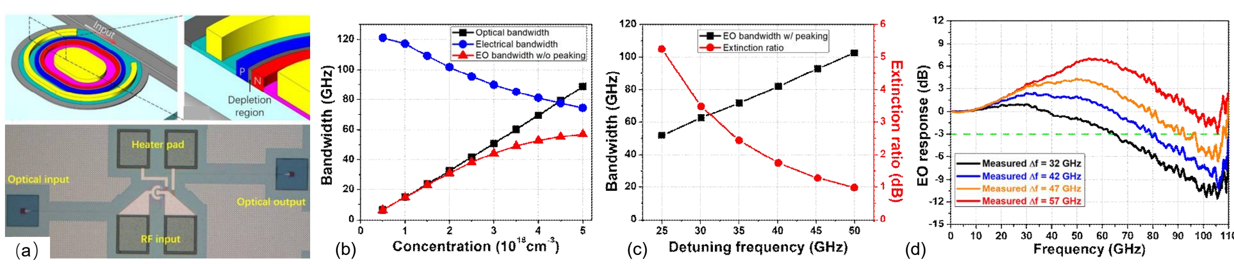

Fig. 1. (a) The schematic for the high-performance MRM. (b) The simulated optical bandwidth, electrical bandwidth and EO bandwidth of the MRM with different doping concentrations, respectively. (c) The simulated EO bandwidth with optical peaking and extinction ratio (ER) of the MRM with different detuning frequency. (d) Measured EO response with 2-V reversed bias voltage.

The schematic of the proposed MRM is presented in Fig 1(a) [8]. The radius of the MRM is designed to be 8 μm. The waveguide width of 420 nm is designed to reduce the propagation loss. We simulated the optical bandwidth, electrical bandwidth and EO bandwidth with different doping concentrations to investigate the relationship between the performance of the MRMs and the doping concentration, as shown in Fig. 1(b). The doping concentration is designed as $3\times10^{18}cm^{-3}$ for the PN junction with the EO bandwidth of 44.3 GHz. Due to the optical peaking of the MRM, the EO bandwidth can be further extended. Figure 1(c) shows the simulated EO bandwidth with optical peaking and ER of the MRM with different detuning frequency. The measured EO response with the detuning frequency Δf of 57 GHz, 47 GHz, 42 GHz, and 32 GHz is shown in Fig. 1(d). To the best of our knowledge, the measured EO bandwidth of 110 GHz is the largest bandwidth ever reported for modulator based on pure-Si waveguide. Base on this MRR, the bit error ratio (BER) for 220 Gb/s PAM-4 and 240 Gb/s PAM-8 after 2-km transmission is calculated to be 1.7×10^{-2} and 1.5×10^{-2}, which meet with the threshold of soft-decision forward error correction (SD-FEC), respectively. More recently, based on the same MRR modulator, the beyond 300 Git/s optical interconnection is experimentally demonstrated with AI acceleration [9].

3. Ge-Si based EAM

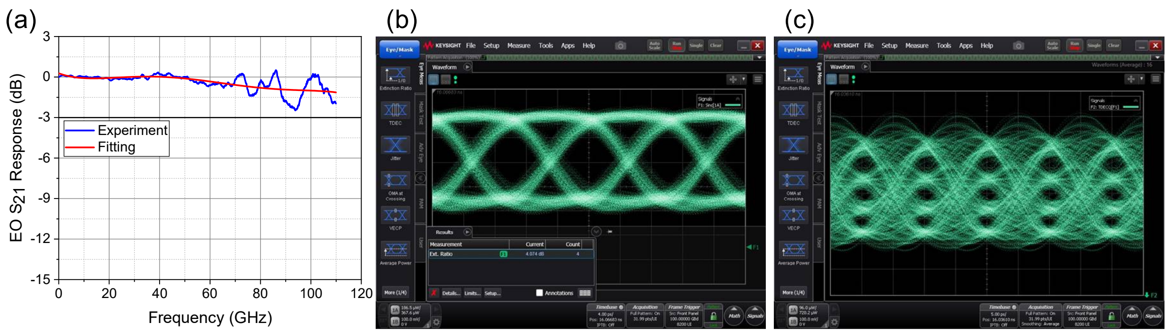

Fig. 2. (a) The RF S_{21} response of the EAM. Measured (b) 100 Gbit/s NRZ and (c) 200 Gbit/s large eye diagrams.

The FK effect intrinsically possesses a sub-picosecond timescales electro-absorption response and enables 100 GHz optical modulation. The working principle of Ge-Si EAM is based on FK effect, according to which the material absorption coefficient is changed by an applied electric field. In OFC 2022, we reported the Ge EAM based on Si-doped lateral p-i-n structure with electro-optic bandwidth beyond 67 GHz [10]. The 110 Gbit/s non-return-to-zero (NRZ) and 160 Gbit/s PAM-4 modulation eye diagrams are demonstrated. However, its modulation efficiency and operation speed need to be further enhanced. By using the double sidewall doped narrow Ge structure (width 600 nm), which is similar to the reported PD in our previous work [11], the electric field in the Ge region is very high. The measured EO 3dB bandwidth at -4.4 V bias is larger than 110 GHz, as shown in Fig. 2(a). Based on this device, the clear and open eye diagrams at 100 Gbit/s NRZ was observed at wavelength of 1600 nm. The dynamic ER can reach to 4 dB. Additionally, the clear opening of the eye diagrams up to 200 Gbit/s four-level pulse amplitude (PAM4) are also achieved without utilizing any digital signal processing, as shown in Fig. 2(c).

4. Ge-Si photodetectors

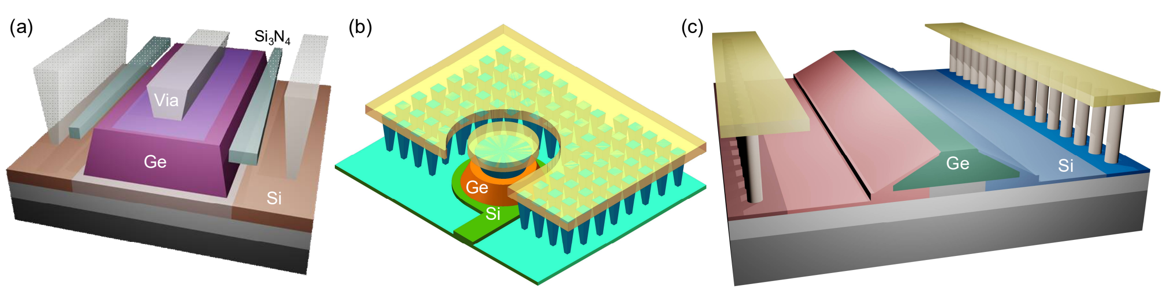

Fig. 3. (a) The Ge-Si PD with double lateral Si_3N_4 waveguides. (b) The light-trapping-structure Ge-Si PD. (c) the sidewall-doped Ge-Si PD.

As shown in Fig. 3(a), we propose the concept of Ge-Si PD with double lateral silicon nitride (Si_3N_4) waveguides, which can serve as a novel waveguide-integrated coupling configuration: double lateral coupling [12]. The Ge-Si PD with double lateral Si_3N_4 waveguides features uniform optical field distribution in the Ge region, which is very beneficial to improving the operation speed for high input power. Under 4 mA photocurrent, a 60 GHz bandwidth operating at -3 V bias is demonstrated. When the photocurrent is up to 12 mA, the 3 dB OE bandwidth still has 36 GHz. With 1 mA photocurrent, the 90, 100, and 105 Gbit/s NRZ and 160, 170, and 180 Gbit/s PAM4 modulation eye diagrams are obtained [12, 13]. The electrical eye diagrams of 60 Gbit/s NRZ under 20 mA photocurrent are also acquired. In order to avoid the metal loss of the Ge region, the light-trapping-structure Ge-Si PD was presented [14], as shown in Fig. 3(b). The light could be constrained in the circular absorption area. The measured 3-dB bandwidth is around 67 GHz, and the responsivity of the PD is around 1.05 A/W. With the aid of offline digital signal processing, the 240 Gbit/s PAM4 signal transmission is achieved. Additionally, we also present a Ge-Si PD in which the sloped sidewalls of Ge are carefully doped [11], as shown in Fig. 3(c). They internal responsivities can reach larger than 1 A/W in the C+L bands. The highest speed of 290 Gbit/s PAM4 and 408 Gbit/s PAM-8 modulation eye diagrams are obtained. The inductive gain peaking technique is demonstrated to be an effective way to boost the bandwidth of Ge-Si PD without sacrificing responsivity [15]. However, the limited bit rate may be attributed to the large signal phase delay with different frequency. Here, by employing the 45 GHz reference (Ref.) PD and carefully designed inductance, the measured 1 dB OE bandwidth of the peaking PD is greater than 67 GHz, as shown in Fig. 4. The deducing and fitting result of 3 dB bandwidth might be 110 GHz. More importantly, it supports the 100 Gbaud PAM8 (300 Gbit/s) large signal reception, which proves the robust of fabricated peaking Ge-Si PD.

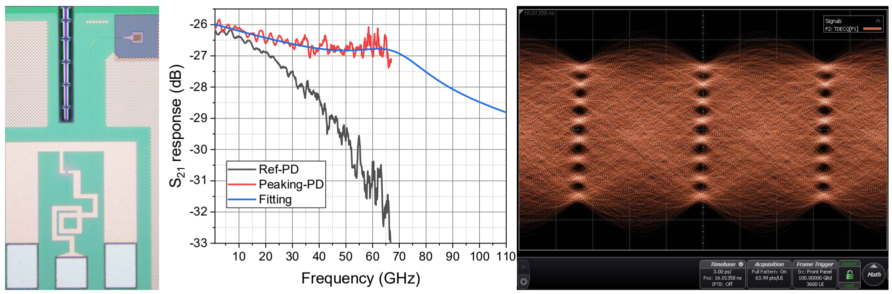

Fig. 4. The optical micrograph, S_{21} response, and eye diagram of the peaking Ge-Si PD.

As shown in Fig. 5, the 1.6 Tbit/s SiPh transceivers including discrete transmitter (Tx) and receiver (Rx) are presented. The Tx and Rx consist of eight channel modulators and PDs, each capable of 200 Gbit/s PAM4 performance (8×200 Gbit/s). At Tx side, the modulator chip is based on the TWE structure with footprints of 4×8.6 mm^2. The Tx and Rx have a 3 dB bandwidth of >45 GHz after advanced packaging.

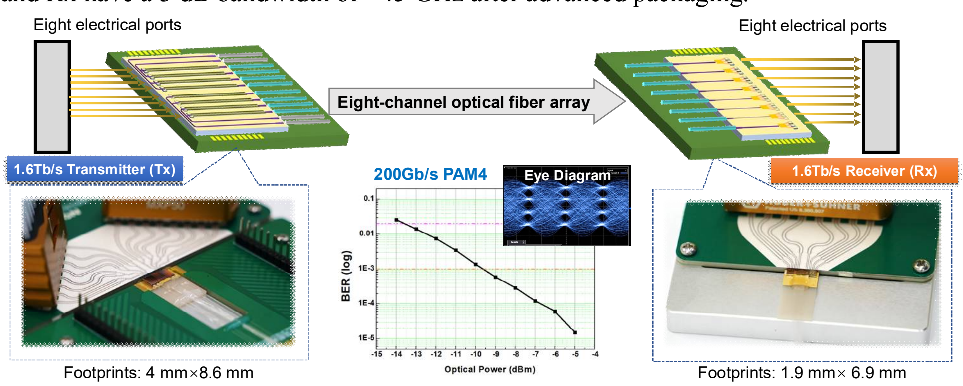

Fig. 5. The 1.6T silicon photonics transceivers.

5. Conclusion

We present our recent progress on the ultrahigh-speed silicon photonic devices, which include the 300 Gbit/s silicon microring modulator, 200 Gbit/s Ge-based EAM and 408 Gbit/s Ge-Si photodetector with the highest bandwidth of 110 GHz. The single-chip 1.6 Tbit/s silicon-based optical transceiver is also demonstrated.

6. Funding: National Natural Science Foundation of China (62205255, U21A20454); Young Top-notch Talent Cultivation Program of Hubei Province.

7. References

[1] D.A.B. Miller, Proc. IEEE 97(7), 1166 (2009).
[2] J. Liu, et al., Nat. Photonics 2(7), 433 (2008).
[3] G. T. Reed, et al., Nat. Photonics 4(8), 518 (2010).
[4] J. Liu, et al., Nat. Photonics 2(7), 433 (2008).
[5] M. S. Alam, et al., Photon. Technol. Lett. 33(24), 1391(2021).
[6] D. Benedikovic, et al., Nanophotonics 10(3), 1059(2021).
[7] S. Lischke, et al., Nat. Photonics 15(12), 925(2021).
[8] Y. Zhang, et al., Photon. Res. 10(4), 1127(2022).
[9] F. Hu, et al., arXiv:2111.05331.
[10] X. Hu, et al., OFC 2022, Th3C.4.
[11] X. Hu, et al., ECOC 2022, Th2E.5.
[12] X. Hu, et al., Photon. Res. 9(5), 749(2021).
[13] X. Hu, et al., Opt. Lett., 46(24), 6019(2021).
[14] D. Chen, et al., Photon. Res. 10(9), 2165(2022).
[15] X. Hu, et al., J. Semicond. 42(2), 020502(2021).